

Vibrations of wind-turbines considering soil-structure interaction

S. Adhikari*¹ and S. Bhattacharya^{2a}

¹College of Engineering, Swansea University, Singleton Park, Swansea SA2 8PP, UK

²Department of Civil Engineering, University of Bristol, 2.37, Queen's Building,
University Walk, Clifton, Bristol, BS8 1TR, UK

(Received January 21, 2010, Accepted July 20, 2010)

Abstract. Wind turbine structures are long slender columns with a rotor and blade assembly placed on the top. These slender structures vibrate due to dynamic environmental forces and its own dynamics. Analysis of the dynamic behavior of wind turbines is fundamental to the stability, performance, operation and safety of these systems. In this paper a simplified approach is outlined for free vibration analysis of these long, slender structures taking the soil-structure interaction into account. The analytical method is based on an Euler-Bernoulli beam-column with elastic end supports. The elastic end-supports are considered to model the flexible nature of the interaction of these systems with soil. A closed-form approximate expression has been derived for the first natural frequency of the system. This new expression is a function of geometric and elastic properties of wind turbine tower and properties of the foundation including soil. The proposed simple expression has been independently validated using an exact numerical method, laboratory based experimental measurement and field measurement of a real wind turbine structure. The results obtained in the paper shows that the proposed expression can be used for a quick assessment of the fundamental frequency of a wind turbine taking the soil-structure interaction into account.

Keywords: mono-pile; natural frequency; beam theory; wind-turbine; soil stiffness.

1. Introduction

It has been estimated that the world will require 50% more energy in 2030 than today (IEA, 2005). With the current policies on fossil fuels, greenhouse gas emissions will be 55% higher driving irreversible climate change and potentially triggering more extreme events such as floods, cyclones, heat waves, change in wind speed. A strategy is required to deliver both energy and climate security without compromising economic growth. Of all the sustainable sources of energy large offshore wind turbines have the proven potential to produce reliable quantities of renewable energy. Potential advantages of offshore turbines include: (a) Limited environmental impacts and out of sight; (b) High wind speed; (c) Available wave/current loading can also be harvested.

Offshore wind turbine can be described as high slenderness low stiffness dynamical system involving complex interaction between the wind, wave and the soil. Due to the variety of cyclic and

* Corresponding Author: Professor, E-mail: s.adhikari@swansea.ac.uk

^aSenior Lecturer

dynamic loadings (arising from the rotor dynamics, out-of-balance masses, varying wind loading intensity, wave loading), cyclic loads are induced in the foundations which are three dimensional in nature. These are relatively new structures and there are no track record of long term performances i.e., 20 years or beyond. Clearly, it is necessary to predict the long term performance of these structures for the energy security from renewable sources.

The design of the foundations for offshore wind turbines remains a challenging task. Fig. 1 shows a schematic diagram of an offshore wind turbine supported on a mono-pile, a particular type of foundation. Mono-pile is a single slender member inserted deep into the ground to support the structure. Typical mono-pile supporting a wind turbine is 3 to 4 m in diameter and 35 to 40 m long. Piles are currently a popular choice for foundations possibly due to its long success in supporting offshore oil platforms. Other forms of foundations that can be used to support wind turbines include suction caissons i.e., an inverted bucket. The performance of suction caissons under the action of static, cyclic and transient has been extensively researched; see for example Byrne and Houlsby (2003).

Currently, monopile foundation design for offshore wind turbines closely follows the pile design for offshore fixed platforms. However, the offshore pile design concepts cannot be directly applied to mono-pile design. There are significant differences between the two pile types:

- Offshore oil platform piles are longer (typically 60 m to 110 m), so degradation effects in the upper soil layers due to cyclic loading are less severe.
- Offshore piles are also significantly restrained from pile head rotation, whereas mono-piles are free-headed.

The issue of cyclic strength degradation of the soil is taken empirically in offshore pile design. In contrast, this is one of the important considerations in mono-pile design. Thus the two loading cases

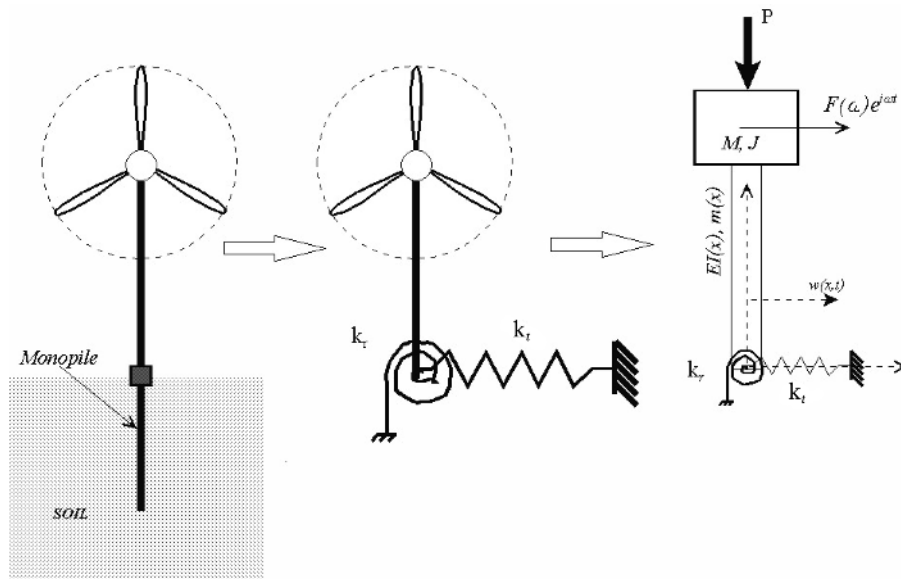


Fig. 1 Mono-pile foundation to support offshore wind turbines and the proposed mathematical model for analysis. The translational spring constant k_t and the rotational spring constant k_r are used to model the soil-structure interaction. Experimental methods to obtain these two constants are discussed later in the paper

are significantly different, and it is not possible to rely on offshore pile design methods, since these might produce an over-conservative or un-conservative design for mono-piles.

A similar problem on cyclic degradation of the soil surrounding a relatively short pile was encountered while designing the next generation offshore FPSO platforms. Fig. 2 shows the degradation concepts due to post-holing as well as possible jetting action due to the one-way cyclic loading on the anchoring piles. These piles are short (typically 20 to 30 m) and the analysis carried out concluded that offshore pile concepts cannot be directly applied. Offshore wind turbine systems (i.e., the combination of rotor-blade-tower-foundation-soil system) are low frequency structures (typical values range between 0.5 Hz to 1.5 Hz) and various loading frequencies from wind, wave and the rotor are also in same orders of magnitude. For example, the predominant frequencies of wind and wave are about 0.1 Hz and the rotor frequencies are in the range of 0.15 to 0.5 Hz. The obvious design issues that stems out of the discussion are as follows:

1. Due to the change in soil characteristics and under the action of cyclic loading, the natural frequency response of the wind turbine system will change constantly. Any change in frequency of the system will call for changes in bending moment and deflection of the top of the tower. This may affect the performance of the overall system and in extreme cases may lead to resonance type failure.

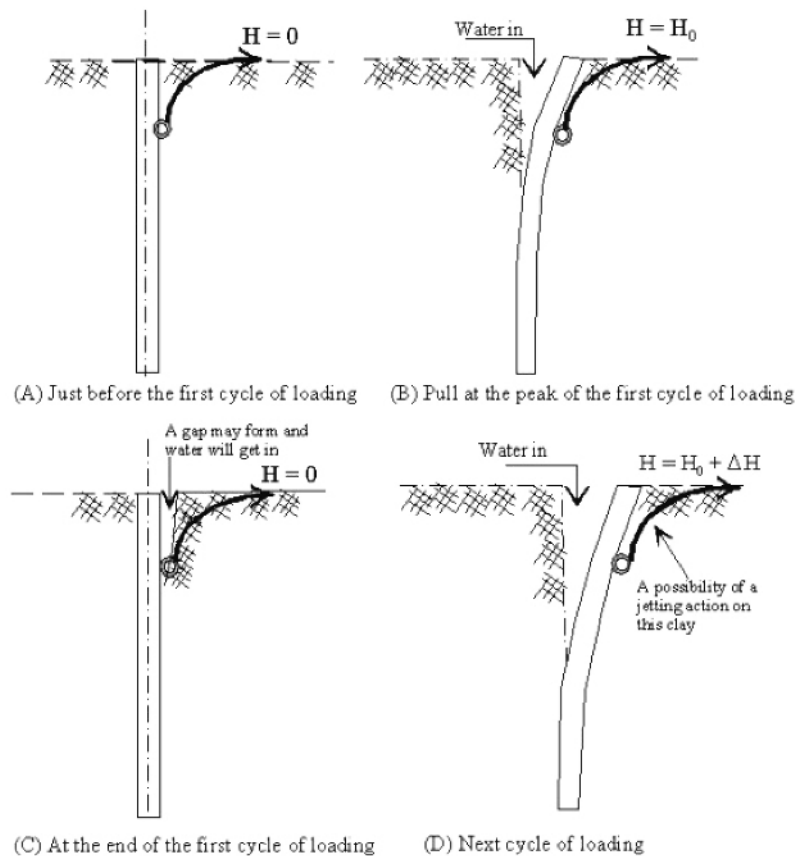


Fig. 2 FPSO Pile-soil interaction subjected to cyclic lateral loading

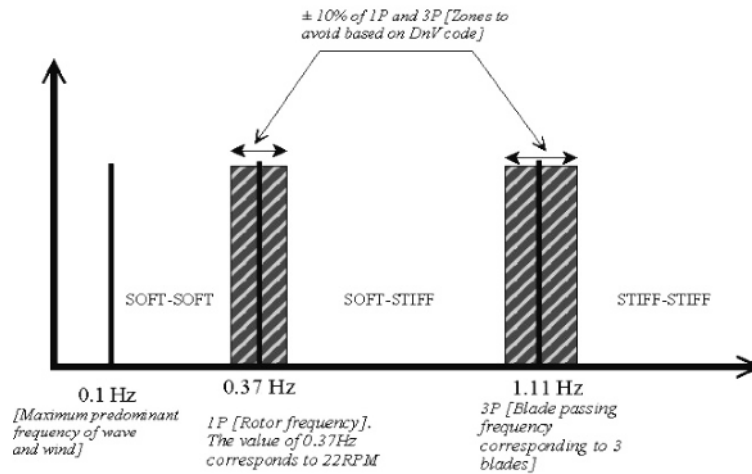


Fig. 3 Various frequencies acting on the wind turbine system

2. Due to climate change, there may be a change in the wave loading, wind speed and more extreme events (such as erratic wind gusts). It is necessary to predict the impact of these short term extreme events.

An obvious solution is to design the wind turbine system so that the natural frequency of the system does not come close to the forcing frequencies. The forcing frequencies are:

1. The frequency due to the wind and the wave
2. The rotor frequency often denoted by 1P
3. The blade passing frequency which is denoted by 2P or 3P depending on the number of blades.

These are shown in Fig. 3. It is of interest to review the DnV code of practice on wind turbines (DnV 2001). The code suggests to design the wind turbine so as to avoid the $\pm 10\%$ zone on either side of the frequencies.

2 Motivation behind the present study

A damped dynamical system with rotating components such as the wind turbine system may lead to nonsymmetric (Adhikari 1999a) and nonproportionally damped (Adhikari 2004) systems. There are specialised software available to carry out the natural frequency analysis of the wind turbines, modal damping and mode shapes at any operating conditions. Some example include GHBLADED (2009) and SAMTECH (2009). Examples of numerical work which includes soil structure interaction can be found in Dash *et al.* (2009). The aim of this paper is to provide a simplified analytical solution which can be used to determine the first natural frequency of the wind turbine system based on back of the envelope calculations. This can help the designer for option engineering i.e., choosing the tower stiffness or the foundation stiffness without the recourse of running a software program. This can also help to physically understand the output from a software program. Tempel and Molenaar (2002) studied the problem by idealising the wind turbine as a flagpole of length L , mass per length m having an average bending stiffness EI with a top mass M . The first natural frequency is given by

$$f_1 \approx \sqrt{\frac{3.04EI}{(M+0.227mL)4\pi^2L^3}} \quad (1)$$

Although they have proposed a simple equation for the first natural frequency, it does not incorporate the flexibility of the foundation. In the previous work Adhikari and Bhattacharya (2011) proposed an exact approach based on the numerical solution of transcendental frequency equation. In this paper we aim to derive simplified approximate expression similar to Eq. (1) by taking the soil-structure interaction into account. Our method evolves from the analytical solution based on idealisation of axially loaded Euler-Bernoulli beam supported on one end by two supports. The beam carries a mass at the free end. This method idealises the wind turbine system by 5 non-dimensional groups and each of which has a physical meaning:

1. Non-dimensional axial load on the tower: To compute this parameter, we need the mass of the blades, rotor and the generator and this differentiates one type of generator/ turbine/blades from the other.
2. Non-dimensional rotary moment of inertia of the system.
3. Non-dimensional overall lateral stiffness of the system: This parameter considers the flexural rigidity of the tower, length of the tower and the lateral stiffness of the foundation. It must be mentioned that the lateral stiffness of the foundation is a function of the soil type and the stiffness of the pile.
4. Non-dimensional rotational stiffness of the system: This parameter considers the flexural rigidity of the tower, length of the tower and the rotational stiffness of the foundation. It must be mentioned that the rotational stiffness of the foundation is a function of the soil type and the stiffness of the pile.
5. Non-dimensional mass ratio: This parameter considers the ratio of the mass of the assembly at the top with that of the tower.

Based on the above non-dimensional values, the first natural frequency of the system can be evaluated based on simple equations to be derived in the paper.

3. Equation of motion and boundary conditions

We consider a typical wind turbine structure as shown in Fig. 1. This system is idealized by an Euler Bernoulli beam. The bending stiffness of the beam is $EI(x)$ and it is resting against the soil. Here x is the spatial coordinate along the height of the structure. The interaction of the structure with the surrounding soil is modeled using two springs. The rotational spring with spring stiffness k_r , and the translational spring with spring stiffness k_t constrains the system at the bottom ($x = 0$). The beam has a top mass M with rotary inertia J with respect to the axis through the center of mass. This top mass is used to idealise the rotor and bladed system. The mass per unit length of the beam is $m(x)$, r is the radius of gyration and the beam is subjected to a constant compressive axial load P . The equation of motion of the beam is given by

$$\frac{\partial^2}{\partial x^2} \left(EI(x) \frac{\partial^2 w(x,t)}{\partial x^2} \right) + \frac{\partial}{\partial x} \left(P \frac{\partial w(x,t)}{\partial x} \right) - \frac{\partial}{\partial x} \left(m(x)r^2 \frac{\partial \ddot{w}(x,t)}{\partial x} \right) + m(x)\ddot{w}(x,t) = f(x,t) \quad (2)$$

Here $w(x, t)$ is the transverse deflection of the beam, t is time, $(\dot{\bullet})$ denotes derivative with respect to time and $f(x, t)$ is the applied time depended and distributed load on the beam. The height of the

structure is considered to be L. An Euler-Bernoulli beam with rotary inertia in Eq. (2) is also known as the Rayleigh beam (Sheu and Yang 2005). Eq. (2) is a fourth-order partial differential equation (Kreyszig 2006) and has been used extensively in literature for various problems, see for example, Abramovich and Hamburger (1991), Adhikari and Bhattacharya (2008), Bhattacharya *et al.* (2009, 2008), Chen (1963), Elishakoff and Johnson (2005), Elishakoff and Perez (2005), Gurgoze (2005a), Gurgoze and Erol (2002), Hetenyi (1946), Huang (1961), Laura and Gutierrez (1986), Oz (2003), Wu and Chou (1998, 1999), Wu and Hsu (2006). Our aim is to obtain the natural frequencies of the system. Here we develop an approach based on the non-dimensionalisation of the equation of motion (2).

Eq. (2) is a quite general equation. It is possible to consider any variation in the bending stiffness $EI(x)$ and mass density $m(x)$ of the structure with height (such as a tapered column). Consideration of such variation normally leads to the case where closed-form solutions are impossible to obtain due to the complex nature of the resulting equations. For simplicity, we therefore assume a special case where all properties are constant along the height of the structure. Noting that the properties are not changing with x , Eq. (2) can be simplified as

$$EI \frac{\partial^4 w(x,t)}{\partial x^4} + P \frac{\partial^2 w(x,t)}{\partial x^2} - mr^2 \frac{\partial^2 \ddot{w}(x,t)}{\partial x^2} + m\ddot{w}(x,t) = f(x,t) \quad (3)$$

The four boundary conditions associated with this equation can be expressed as

· Bending moment at $x = 0$

$$EI \frac{\partial^2 w(x,t)}{\partial x^2} - k_r \frac{\partial w(x,t)}{\partial x} = 0|_{x=0} \quad \text{or} \quad EIw''(0,t) - k_r w'(0,t) = 0 \quad (4)$$

· Shear force at $x = 0$

$$EI \frac{\partial^3 w(x,t)}{\partial x^3} + P \frac{\partial w(x,t)}{\partial x} + k_t w(x,t) - mr^2 \frac{\partial \ddot{w}(x,t)}{\partial x} = 0|_{x=0} \quad (5)$$

$$\text{or} \quad EIw'''(0,t) + Pw'(0,t) + k_t w(0,t) - mr^2 \frac{\partial \ddot{w}(0,t)}{\partial x} = 0$$

· Bending moment at $x = L$

$$EI \frac{\partial^2 w(x,t)}{\partial x^2} + J \frac{\partial \ddot{w}(x,t)}{\partial x} = 0|_{x=L} \quad \text{or} \quad EIw''(L,t) + J \frac{\partial \ddot{w}(L,t)}{\partial x} = 0 \quad (6)$$

· Shear force at $x = L$

$$EI \frac{\partial^3 w(x,t)}{\partial x^3} + P \frac{\partial w(x,t)}{\partial x} - M\ddot{w}(x,t) - mr^2 \frac{\partial \ddot{w}(x,t)}{\partial x} = 0|_{x=L} \quad (7)$$

$$EIw'''(L,t) + Pw'(L,t) + M\ddot{w}(L,t) - mr^2 \frac{\partial \ddot{w}(L,t)}{\partial x} = 0$$

Assuming harmonic solution (the separation of the variables) we have

$$w(x,t) = W(\xi) \exp\{i\omega t\}, \quad f(x,t) = F(\xi) \exp\{i\omega t\} \quad \xi = x/L \quad (8)$$

Substituting this in the equation of motion and the boundary conditions, Eqs. (3) - (7), results

$$\frac{EI d^4 W(\xi)}{L^4 d\xi^4} + \frac{P d^2 W(\xi)}{L^2 d\xi^2} - m\omega^2 W(\xi) + \frac{mr^2\omega^2 d^2 W(\xi)}{L^2 d\xi^2} = F(\xi) \quad (9)$$

$$\frac{EI}{L^2} W''(0) - \frac{k_r}{L} W'(0) = 0 \quad (10)$$

$$\frac{EI}{L^3} W'''(0) + \frac{P}{L} W'(0) + k_t W(0) + \frac{mr^2\omega^2}{L} W'(0) = 0 \quad (11)$$

$$\frac{EI}{L^2} W''(1) - \frac{\omega^2 J}{L} W'(1) = 0 \quad (12)$$

$$\frac{EI}{L^3} W'''(1) + \frac{P}{L} W'(1) + \omega^2 M W(1) + \frac{mr^2\omega^2}{L} W'(1) = 0 \quad (13)$$

It is convenient to express these equations in terms of non-dimensional parameters by elementary rearrangements as

$$\frac{d^4 W(\xi)}{d\xi^4} + \tilde{\nu} \frac{d^2 W(\xi)}{d\xi^2} - \Omega^2 W(\xi) = F(\xi) L^4 / EI \quad (14)$$

$$W''(0) - \eta_r W'(0) = 0 \quad (15)$$

$$W'''(0) + \tilde{\nu} W'(0) + \eta_t W(0) = 0 \quad (16)$$

$$W''(1) - \beta \Omega^2 W'(1) = 0 \quad (17)$$

$$W'''(1) + \tilde{\nu} W'(1) + \alpha \Omega^2 W(1) = 0 \quad (18)$$

where

$$\tilde{\nu} = \nu + \mu^2 \Omega^2 \quad (19)$$

and

$$\nu = \frac{PL^2}{EI} \quad (\text{nondimensional axial force}) \quad (20)$$

$$\eta_r = \frac{k_r L}{EI} \quad (\text{nondimensional rotational end stiffness}) \quad (21)$$

$$\eta_t = \frac{k_t L^3}{EI} \quad (\text{nondimensional translational end stiffness}) \quad (22)$$

$$\Omega^2 = \omega^2 \frac{mL^4}{EI} \quad (\text{nondimensional frequency parameter}) \quad (23)$$

$$\alpha = \frac{M}{mL} \quad (\text{mass ratio}) \quad (24)$$

$$\beta = \frac{J}{mL^3} \quad (\text{nondimensional rotary inertia}) \quad (25)$$

$$\mu = \frac{r}{L} \quad (\text{nondimensional radius of gyration}) \quad (26)$$

For most columns $\mu = r/L \ll 1$ so that $\mu^2 \approx 0$. As a result for low frequency vibration one expects $\tilde{\nu} \approx \nu$. For notational convenience we define the natural frequency scaling parameter

$$c_0 = \sqrt{\frac{EI}{mL^4}} \quad (27)$$

Using this, from Eq. (23) the natural frequencies of the system can be obtained as

$$\omega_j = \Omega_j c_0; \quad j = 1, 2, 3, \dots \quad (28)$$

4. Exact equation of the natural frequencies

Natural frequencies of the system can be obtained from the 'free vibration problem' by considering no force on the system. Therefore, we consider $f(x, t) = 0$ in the subsequent analysis. Assuming a solution of the form

$$W(\xi) = \exp\{\lambda \xi\} \quad (29)$$

and substituting eq. (14) results

$$\lambda^4 + \tilde{\nu} \lambda^2 - \Omega^2 = 0 \quad (30)$$

This equation is often known as the frequency equation or dispersion relationship. This is the equation governing the natural frequencies of the beam. Solving this equation for λ^2 we have

$$\lambda^2 = -\frac{\tilde{\nu}}{2} \pm \sqrt{\left(\frac{\tilde{\nu}}{2}\right)^2 + \Omega^2} = -\left(\sqrt{\left(\frac{\tilde{\nu}}{2}\right)^2 + \Omega^2} + \frac{\tilde{\nu}}{2}\right), \left(\sqrt{\left(\frac{\tilde{\nu}}{2}\right)^2 + \Omega^2} - \frac{\tilde{\nu}}{2}\right) \quad (31)$$

Because $\tilde{\nu}^2$ and Ω^2 are always positive quantities, both roots are real with one negative and one positive root. Therefore, the four roots can be expressed as

$$\lambda = \pm i \lambda_1, \pm \lambda_2 \quad (32)$$

where

$$\lambda_1 = \left(\sqrt{\left(\frac{\tilde{\nu}}{2}\right)^2 + \Omega^2} + \frac{\tilde{\nu}}{2}\right)^{1/2} \quad (33)$$

$$\text{and } \lambda_2 = \left(\sqrt{\left(\frac{\tilde{\nu}}{2}\right)^2 + \Omega^2} - \frac{\tilde{\nu}}{2}\right)^{1/2} \quad (34)$$

From Eqs. (33) and (34) also note that

$$\lambda_1^2 - \lambda_2^2 = \tilde{\nu} \quad (35)$$

In view of the roots in Eq. (32) the solution $W(\xi)$ can be expressed as

$$W(\xi) = a_1 \sin \lambda_1 \xi + a_2 \cos \lambda_1 \xi + a_3 \sinh \lambda_2 \xi + a_4 \cosh \lambda_2 \xi$$

$$\text{or } W(\xi) = \mathbf{s}^T(\xi) \mathbf{a} \quad (36)$$

where the vectors

$$\mathbf{s}(\xi) = \{\sin \lambda_1 \xi, \cos \lambda_1 \xi, \sinh \lambda_2 \xi, \cosh \lambda_2 \xi\}^T \quad (37)$$

$$\text{and } \mathbf{a} = \{a_1, a_2, a_3, a_4\}^T \quad (38)$$

are defined as above.

Applying the boundary conditions in Eqs. (15) - (18) on the expression of $W(\xi)$ in (36) we have

$$\mathbf{R} \mathbf{a} = \mathbf{0} \quad (39)$$

where the matrix \mathbf{R} is defined as

$$\mathbf{R} = \begin{bmatrix} s_1''(0) - \eta_r s_1'(0) & s_2''(0) - \eta_r s_2'(0) \\ s_1'''(0) + \tilde{\nu} s_1'(0) + \eta_r s_1(0) & s_2'''(0) + \tilde{\nu} s_2'(0) + \eta_r s_2(0) \\ s_1''(1) - \beta \Omega^2 s_1'(1) & s_2''(1) - \beta \Omega^2 s_2'(1) \\ s_1'''(1) + \tilde{\nu} s_1'(1) + \alpha \Omega^2 s_1(1) & s_2'''(1) + \tilde{\nu} s_2'(1) + \alpha \Omega^2 s_2(1) \\ s_3''(0) - \eta_r s_3'(0) & s_4''(0) - \eta_r s_4'(0) \\ s_3'''(0) + \tilde{\nu} s_3'(0) + \eta_r s_3(0) & s_4'''(0) + \tilde{\nu} s_4'(0) + \eta_r s_4(0) \\ s_3''(1) - \beta \Omega^2 s_3'(1) & s_4''(1) - \beta \Omega^2 s_4'(1) \\ s_3'''(1) + \tilde{\nu} s_3'(1) + \alpha \Omega^2 s_3(1) & s_4'''(1) + \tilde{\nu} s_4'(1) + \alpha \Omega^2 s_4(1) \end{bmatrix} \quad (40)$$

Substituting functions $s_j(\xi), j = 1, \dots, 4$ from Eq. (37) and simplifying we obtain

$$\mathbf{R} = \begin{bmatrix} -\lambda_1 \eta_r & -\lambda_1^2 \\ \lambda_1^3 + \nu \lambda_1 & \eta_t \\ -\sin(\lambda_1) \lambda_1^2 - \Omega^2 \beta \cos(\lambda_1) \lambda_1 & -\cos(\lambda_1) \lambda_1^2 - \Omega^2 \beta \sin(\lambda_1) \lambda_1 \\ -\cos(\lambda_1) \lambda_1^3 + \tilde{\nu} \cos(\lambda_1) \lambda_1 + \Omega^2 \alpha \sin(\lambda_1) \sin(\lambda_1) \lambda_1^3 + \tilde{\nu} \sin(\lambda_1) \lambda_1 + \Omega^2 \alpha \cos(\lambda_1) \\ -\lambda_2 \eta_r & \lambda_2^2 \\ \lambda_2^3 + \nu \lambda_2 & \eta_t \\ \sinh(\lambda_2) \lambda_2^2 - \Omega^2 \beta \cosh(\lambda_2) \lambda_2 & \cosh(\lambda_2) \lambda_2^2 - \Omega^2 \beta \sinh(\lambda_2) \lambda_2 \\ \cosh(\lambda_2) \lambda_2^3 + \tilde{\nu} \cos(\lambda_2) \lambda_2 + \Omega^2 \alpha \sinh(\lambda_2) \sinh(\lambda_2) \lambda_2^3 + \tilde{\nu} \sinh(\lambda_2) \lambda_2 + \Omega^2 \alpha \cosh(\lambda_2) \end{bmatrix} \quad (41)$$

In order to have nontrivial solutions of the homogenous in eq. (39), the determinant of the

coefficients matrix should be zero, leading to the frequency equation

$$|\mathbf{R}| = 0 \quad (42)$$

The natural frequencies can be obtained by solving Eq. (42) for Ω . Due to the complexity of this transcendental equation it should be solved numerically. The details of the above can be found in Adhikari and Bhattacharya (2011).

5. Approximate expression of the natural frequency

In the previous section exact expressions for the equation of the natural frequencies of the combine wind turbine-soil system have been derived. Since only numerical solutions to these transcendental equations are available, in this section we aim to derive approximate closed-form solution with the aim of gaining more physical insights. For this application, the first mode of vibration is the most significant. As a result, we focus our attention on the first mode only.

In the first mode we can replace the distributed system by a single-degree-of-freedom system with equivalent stiffness k_e and equivalent mass M_e as shown in Fig. 4. The first natural frequency is given by

$$\omega_1^2 = \frac{k_e}{M_e} \quad (43)$$

Following Table 8-8, case 1, page 158 of (Blevins 1984) for a cantilever beam carrying a tip mass M , one has

$$M_e = M + 0.24M_b = (\alpha + 0.24)mL \quad (44)$$

Representation of a cantilevered beam carrying a tip mass by an equivalent spring-mass system has been discussed by Gurgoze (2005b). For our case the beam is resting on elastic foundation and also have an end force. Therefore the coefficient 0.24 needs to be modified to take these effects into account. We suppose that the equivalent mass can be represented by

$$M_e = (\alpha + \gamma_m)mL \quad (45)$$

where γ_m is the mass correction factor.

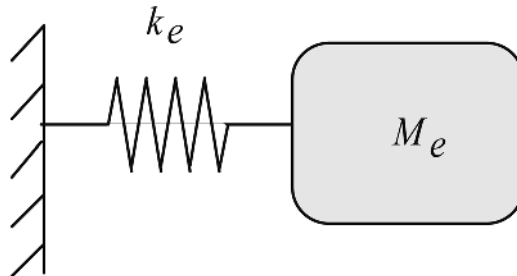


Fig. 4 Equivalent single-degree-of-freedom system for the first bending mode of the wind turbine

It is often useful to express k_e in terms of the equivalent end stiffness of a cantilever beam, $k_{CL} = 3EI/L^3$. Therefore, the first natural frequency can be expressed as

$$\omega_1^2 \approx \frac{k_e}{M_e} = \frac{k_e}{k_{CL}(\alpha + \gamma_m)mL} = \frac{EI}{mL^4} \frac{3\gamma_k}{(\alpha + \gamma_m)} \quad (46)$$

$$\text{or } \omega_1 \approx c_0 \sqrt{\frac{3\gamma_k}{\alpha + \gamma_m}} \quad (47)$$

where the stiffness correction factor γ_k is defined as

$$\gamma_k = \frac{k_e}{k_{CL}} \quad (48)$$

We only need to obtain γ_k and γ_m in order to apply the expression of the first natural frequency in eq. (46).

5.1 Determination of the stiffness correction factor

The equivalent stiffness in the first-mode is calculated by applying a unit static load to the free end of the wind turbine and calculating the deflection under this load. For the static problem the rotary inertia of the end-mass and the wind turbine can be neglected. The static equation and the associated boundary conditions can be obtained as special cases of Eqs. (3)-(7). Considering a constant static lateral force F is applied at $x = L$ on the beam, the equation of static equilibrium can be expressed as

$$EI \frac{d^4 w(x)}{dx^4} + P \frac{d^2 w(x)}{dx^2} = 0 \quad (49)$$

The four boundary conditions associated with the above equation can be expressed as

· Bending moment at $x = 0$

$$EI \frac{d^2 w(x)}{dx^2} - k_r \frac{dw(x)}{dx} = 0 \Big|_{x=0} \text{ or } EI w''(0) - k_r w'(0) = 0 \quad (50)$$

· Shear force at $x = 0$

$$EI \frac{d^3 w(x)}{dx^3} + P \frac{dw(x)}{dx} + k_t w(x, t) = 0 \Big|_{x=0} \text{ or } EI w'''(0) + P w'(0) + k_t w(0) = 0 \quad (51)$$

· Bending moment at $x = L$

$$\frac{d^2 w(x)}{dx^2} = 0 \Big|_{x=L} \text{ or } w''(L) = 0 \quad (52)$$

· Shear force at $x = L$

$$EI \frac{d^3 w(x)}{dx^3} + P \frac{dw(x)}{dx} - F = 0 \Big|_{x=L} \text{ or } EI w'''(L) + P w'(L) + F = 0 \quad (53)$$

Using the non-dimensional length variable ξ and following the procedure outlined in the previous section the governing equation boundary conditions can be expressed as

$$\frac{d^4 W(\xi)}{d\xi^4} + \nu \frac{d^2 W(\xi)}{d\xi^2} = 0 \quad (54)$$

$$W''(0) - \eta_r W'(0) = 0 \quad (55)$$

$$W'''(0) + \nu W'(0) + \eta_t W(0) = 0 \quad (56)$$

$$W'(1) = 0 \quad (57)$$

$$W'''(1) + \nu W'(1) = -\frac{FL^3}{EI} \quad (58)$$

Considering a trial solution of the form in eq. (29) and substituting in the governing eq. (54) results

$$\lambda^4 + \nu \lambda^2 = 0 \text{ or } \lambda^2(\lambda^2 + \nu) = 0 \quad (59)$$

Solving this equation for λ^2 we have

$$\lambda^2 = 0 \text{ and } \lambda = \pm i\sqrt{\nu} \quad (60)$$

In view of the roots in in eq. (60) the solution $W(\xi)$ can be expressed as

$$W(\xi) = c_1 + c_2 \xi + c_3 \sin \lambda \xi + c_4 \cos \lambda \xi \text{ or } W(\xi) = \mathbf{s}^T(\xi) \mathbf{c} \quad (61)$$

where the vectors

$$\mathbf{s}(\xi) = \{1, \xi, \sin \lambda \xi, \cos \lambda \xi\}^T \quad (62)$$

$$\text{and } \mathbf{c} = \{c_1, c_2, c_3, c_4\}^T. \quad (63)$$

Applying the boundary conditions in eqs. (55) - (58) on the expression of $W(\xi)$ in (61) we have

$$\mathbf{Q} \mathbf{c} = \mathbf{f} \quad (64)$$

where

$$\mathbf{f} = \begin{Bmatrix} 0 \\ 0 \\ 0 \\ \frac{FL^3}{EI} \end{Bmatrix} \quad (65)$$

and the matrix

$$\mathbf{Q} = \begin{bmatrix} 0 & -\eta_r & -\eta_r \lambda & -\lambda^2 \\ \eta_t & \nu & -\lambda^3 + \nu \lambda & \eta_t \\ 0 & 0 & -\sin(\lambda) \lambda^2 & -\cos(\lambda) \lambda^2 \\ 0 & \nu & \cos(\lambda) \lambda (-\lambda^2 + \nu) & -\sin(\lambda) \lambda (-\lambda^2 + \nu) \end{bmatrix}. \quad (66)$$

The expression of \mathbf{Q} is obtained by substituting the functions $s_j(\xi)$, $j = 1, \dots, 4$ from eq. (62). The constants c_j can be obtained from eq. (64) as

$$\mathbf{c} = \mathbf{Q}^{-1} \mathbf{f} \quad (67)$$

The deflection at the free end δ_L can be obtained by substituting $\xi = 1$ in eq. (61) as

$$\delta_L = W(1) = \mathbf{s}^T(1) \mathbf{c} = \mathbf{s}^T(1) \mathbf{Q}^{-1} \mathbf{f} \quad (68)$$

The equivalent stiffness k_e can be obtained using

$$k_e = \frac{F}{\delta_L} = \frac{F}{(\mathbf{s}^T(1) \mathbf{Q}^{-1} \mathbf{f})} \quad (69)$$

and consequently the stiffness correction factor defined in eq. (48) can be calculated as

$$\gamma_k = \frac{k_e}{k_{CL}} = \frac{F L^3}{\delta_L 3EI} = \frac{1}{3} \frac{\lambda^3 \eta_t (\eta_r \cos(\lambda) - \lambda \sin(\lambda))}{\eta_r \eta_t (\sin(\lambda) - \lambda \cos(\lambda)) + \lambda^2 (\eta_t \sin(\lambda) + \eta_r \cos(\lambda) - \lambda^2 \sin(\lambda))} \quad (70)$$

The above expression of γ_k is quite general as it considers both the affect of axial load and support stiffness. It is interesting to consider some special cases

· *No axial force, $\nu = 0$:*

$$\lim_{\lambda \rightarrow 0} \gamma_k = \frac{\eta_r \eta_t}{3 \eta_r + \eta_r \eta_t + 3 \eta_t} \quad (71)$$

· *The system is completely restrained against rotation*

$$\lim_{\eta_r \rightarrow \infty} \gamma_k = 1/3 \frac{\eta_t \cos(\lambda) \lambda^3}{\cos(\lambda) \lambda^3 + \eta_t \sin(\lambda) - \lambda \eta_t \cos(\lambda)} \quad (72)$$

· *The system is completely restrained against translation*

$$\lim_{\eta_t \rightarrow \infty} \gamma_k = -1/3 \frac{\lambda^3 (-\sin(\lambda) \lambda + \eta_r \cos(\lambda))}{-\sin(\lambda) \lambda^2 - \eta_r \sin(\lambda) + \lambda \eta_r \cos(\lambda)} \quad (73)$$

The value of γ_k calculated from eq. (70) can be substituted into eq. (47) to obtain the first natural frequency of the coupled wind turbine-soil system. The value of γ_k given by eq. (70) cover the complete parametric space of η_r , η_t and ν .

In Fig. 5, the overall variation of the stiffness correction factor γ_k of the wind turbine with respect

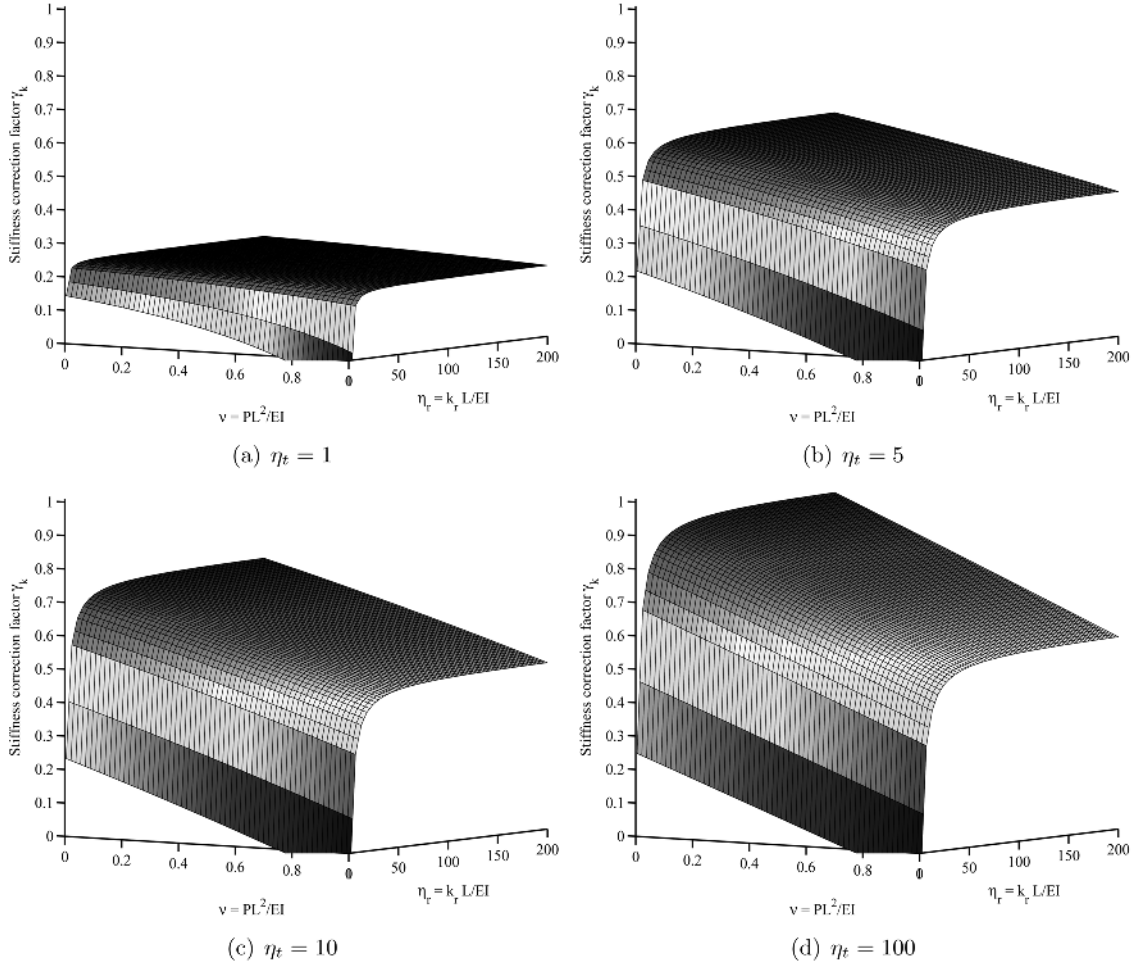


Fig. 5 The variation of the stiffness correction factor γ_k of the wind turbine with respect to the nondimensional axial load ν and nondimensional rotational soil stiffness η_r . Four fixed values of the nondimensional translational stiffness η_t are considered in the four subplots

to both nondimensional rotational soil stiffness and axial load is shown in a 3D plot. Four fixed values of the nondimensional translational stiffness η_t are considered in the four subplots. The interesting feature to observe from this plot are (a) the rapid and sharp ‘fall’ in the natural frequency for small values of η_r , and relative flatness for values of η_r approximately over 50, and (b) extremely high sensitivity for lower values of ν . The parameter η_t has an overall ‘scaling effect’ of the natural frequency. Higher values of the stiffness corresponds to higher values of the natural frequency as expected. In Fig. 6, the overall variation of the stiffness correction factor γ_k with respect to both the nondimensional soil stiffness parameters is shown in a 3D plot. Four fixed values of the nondimensional axial load ν are considered in the four subplots. It can be seen that lower values of ν corresponds to higher values of the natural frequency as seen in the previous figures. These plots can be used to understand the overall design of the system.

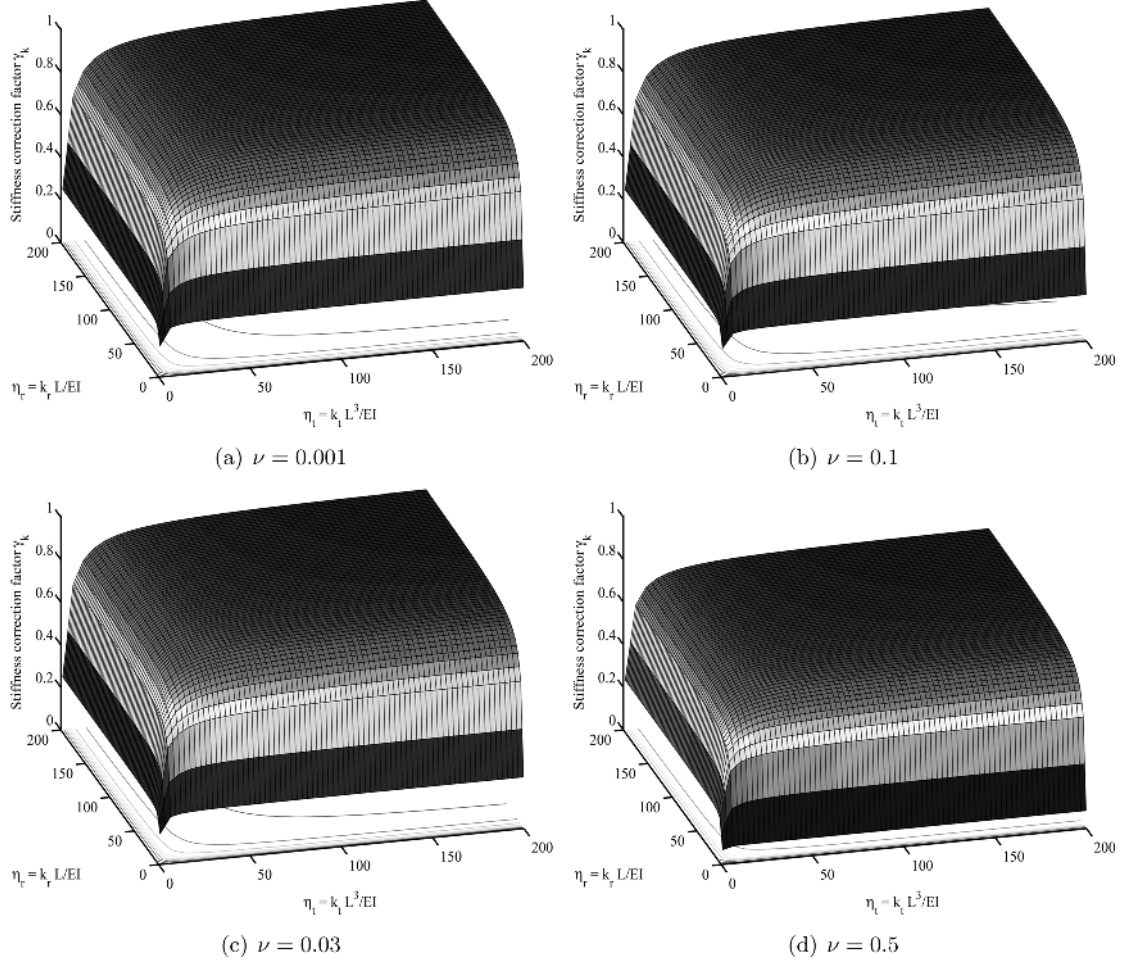


Fig. 6 The variation of the stiffness correction factor γ_k of the wind turbine with respect to the nondimensional translational stiffness η_t and nondimensional rotational soil stiffness η_r . Four fixed values of the nondimensional axial load ν are considered in the four subplots

5.2 Determination of the mass correction factor

From the physics of the problem we note that the axial force within the beam will have very little influence on the equivalent mass. Therefore, neglecting the axial load, the equation of dynamic equilibrium can be expressed as

$$EI \frac{\partial^4 w(x, t)}{\partial x^4} + m \frac{\partial^2 w(x, t)}{\partial t^2} = 0 \quad (74)$$

To obtain the equivalent mass, we perturb the system by unit displacement amplitude at the free end so that $w(L, t) = 1$. This choice of unity is for mathematical convenience in the calculation of the kinetic energy. The results derived in the section is independent of this choice. Assuming

standard harmonic solution as in eq. (8), the equation of motion and the four associated boundary conditions can be expressed as

$$\frac{d^4 W(\xi)}{d\xi^4} - \Omega^2 W(\xi) = 0 \quad (75)$$

$$W''(0) - \eta_r W'(0) = 0 \quad (76)$$

$$W'''(0) + \eta_t W(0) = 0 \quad (77)$$

$$W''(1) = 0 \quad (78)$$

$$W(1) = 1 \quad (79)$$

We use the static deflection shape as the trial solution. Therefore, $W(\xi)$ can be expressed as

$$W(\xi) = \mathbf{s}^T(\xi) \mathbf{c} \quad (80)$$

where the vectors

$$\mathbf{s}(\xi) = \{1, \xi, \xi^2, \xi^3\}^T \quad (81)$$

$$\text{and } \mathbf{c} = \{c_1, c_2, c_3, c_4\}^T \quad (82)$$

Applying the boundary conditions in eqs. (76) - (79) on the expression of $W(\xi)$ in (80) we have

$$\mathbf{Q} \mathbf{c} = \mathbf{f} \quad (83)$$

where

$$\mathbf{f} = \begin{Bmatrix} 0 \\ 0 \\ 0 \\ 1 \end{Bmatrix} \quad (84)$$

and the matrix

$$\mathbf{Q} = \begin{bmatrix} 0 & -\eta_r & 2 & 0 \\ \eta_t & 0 & 0 & 6 \\ 0 & 0 & 2 & 6 \\ 1 & 1 & 1 & 1 \end{bmatrix} \quad (85)$$

The expression of \mathbf{Q} is obtained by substituting the functions $s_j(\xi)$, $j = 1, \dots, 4$ from eq. (81). The constants c_j can be obtained from eq. (83) as

$$\mathbf{c} = \mathbf{Q}^{-1} \mathbf{f} \quad (86)$$

Considering harmonic motion as in eq. (8), the kinetic energy of the beam can be obtained as

$$\begin{aligned}
 T &= \frac{\omega^2}{2} \int_0^L m W^2(x) dx + \frac{\omega^2}{2} M W^2(L) \\
 &= mL \frac{\omega^2}{2} \int_0^1 W^T(\xi) W(\xi) d\xi + \frac{\omega^2}{2} M 1^2 \\
 &= mL \frac{\omega^2}{2} \int_0^1 \mathbf{c}^T \mathbf{s}(\xi) \mathbf{s}^T(\xi) \mathbf{c} d\xi + \frac{\omega^2}{2} M \\
 &= \frac{\omega^2}{2} (mL \gamma_m + M)
 \end{aligned} \tag{87}$$

where the mass correction factor is given by

$$\gamma_m = \int_0^1 \mathbf{c}^T \mathbf{s}(\xi) \mathbf{s}^T(\xi) \mathbf{c} d\xi \tag{88}$$

Evaluating this integral we have

$$\gamma_m = \frac{3}{140} \frac{11 \eta_r^2 \eta_t^2 + 77 \eta_t^2 \eta_r + 105 \eta_r^2 \eta_t + 140 \eta_t^2 + 420 \eta_r \eta_t + 420 \eta_r^2}{9 \eta_r^2 + 6 \eta_r^2 \eta_t + 18 \eta_r \eta_t + \eta_r^2 \eta_t^2 + 6 \eta_t^2 \eta_r + 9 \eta_t^2} \tag{89}$$

In Fig. 7 the parametric variation of of the mass correction factor γ_m of a cantilever wind turbine with respect to both the nondimensional soil stiffness parameters is shown in a 3D plot. It is interesting to consider the special case when the support is completely restrained. Taking the limit $\eta_r \rightarrow \infty$ and $\eta_t \rightarrow \infty$ we have

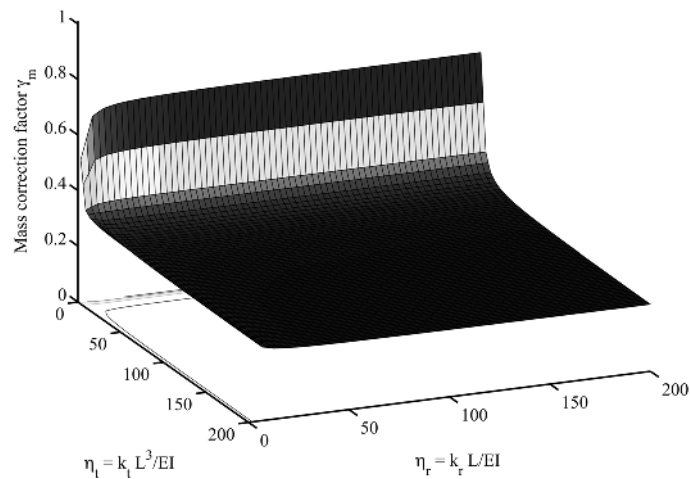


Fig. 7 The variation of the mass correction factor γ_m of the wind turbine with respect to the nondimensional translational stiffness η_t and nondimensional rotational soil stiffness η_r .

$$\lim_{\eta_r \rightarrow \infty, \eta_t \rightarrow \infty} \gamma_m = \frac{33}{140} = 0.2357 \quad (90)$$

which agrees exactly with Table 8-8, case 1, page 158 of Blevins (1984). This analysis shows that the expression of γ_m is the generalization of the classical case so that it considers the effect of elastic foundation.

6. Validation and practical applications of the proposed approach

6.1 Numerical validation

In this section we aim to validate the approximate expressions developed against the exact results. First we determine the relevant non-dimensional parameters in the equations derived here. We focus our attention on the affect of ν and the non-dimensional foundation rotational stiffness η_r on the first-natural frequency. For this reason, the numerical results are presented as a function of ν and η_r . These two parameters are considered because the boundary condition and the load of the turbine are the crucial design issues for the overall system.

The non-dimensional mass ratio can be obtained as

$$\alpha = \frac{M}{mL} = \frac{P}{gmL} = \frac{PL^2}{EI} \left(\frac{EI}{gmL^3} \right) = \nu \left(\frac{EI}{mL^4} \right) L/g = \nu c_0^2 L/g \quad (91)$$

We consider the rotary inertia of the blade assembly $J = 0$. This is not a very bad assumption if there is very less misalignment.

In this example we have used the data of a wind turbine given by Tempel and Molenaar (2002). The numerical values of the main parameters are summarised in Table 1. The moment of inertia of the circular cross section can be obtained as

$$I = \frac{\pi}{64} D^4 - \frac{\pi}{64} (D - t_h)^4 \approx \frac{1}{16} \pi D^3 t_h = 0.6314 m^4 \quad (92)$$

Table 1 Material and geometric properties of the turbine structure

Turbine Structure Properties	Numerical values
Length (L)	81 m
Average diameter (D)	3.5 m
Thickness (t_h)	0.075 mm
Mass density (ρ)	7800 kg/m ³
Young's modulus (E)	2.1 × 10 ¹¹ Pa
Mass density (ρ_t)	7800 kg/m ³
Rotational speed (ϖ)	22 r.p.m = 0.37 Hz
Top mass (M)	130,000 kg
Rated power	3 MW

The mass density per unit length of the system can be obtained as

$$m = \rho A \approx \rho \pi D t_h / 2 = 3.1817 \times 10^3 \text{ kg/m} \quad (93)$$

Using these, the mass ratio $\alpha = 0.2495$ and the nondimensional axial force $\nu = 0.0652$. We also obtain the natural frequency scaling parameter can be obtained as

$$c_0 = \frac{EI}{mL^4} = 0.9682 \text{ s}^{-1} \quad (94)$$

Since no information on the rotary inertia of the blade assembly is given, we consider $J = 0$. This approximation is likely cause insignificant error for the first natural frequency. The radius of gyration of the wind turbine is given by

$$r = \sqrt{\frac{I}{A}} = \frac{1}{4} \sqrt{D^2 + (D - t_h)^2} \approx \frac{D}{2\sqrt{2}} = 1.2374m \quad (95)$$

Therefore, the nondimensional radius of gyration $\mu = r/L = 0.0151$. From Eq. (19) we therefore have

$$\tilde{\nu} = \nu + 2.2844 \times 10^{-4} \Omega^2 \approx \nu \quad (96)$$

The values of the soil stiffness parameters were not given. For the fixed support, the values of η_r and η_t will be infinity. Therefore, we will use η_r and η_t as variable parameters and try to understand how they affect the overall approximation obtained using the proposed approach.

We substitute the derived constants in Eqs. (33) and (34) to obtain λ_1 and λ_2 . Substituting them in Eq. (42) we solve for the nondimensional first natural frequency Ω_1 in Matlab[®]. For most applications the first natural frequency is the most important as the excitation frequency is generally between 0.1 - 0.9 Hz. Higher natural frequencies can however be obtained by solving Eq. (42).

Approximation of the first natural frequency of the wind turbine with respect to the axial load for different values of nondimensional rotational soil stiffness and four fixed values of the nondimensional translational stiffness are shown in Fig. 8. A similar plot, showing the approximation of the first natural frequency with respect to the nondimensional translational soil stiffness for different values of axial force and four fixed values of the nondimensional rotational stiffness is given by Fig. 9.

6.2 Experimental validation

Numerical results in the previous section shows the validity of the proposed approximate expression for the natural frequency. In this section we validated this expression against laboratory based experimental results. In order to validate the proposed method, one needs to obtain η_r , η_t and the natural frequency for the experimental wind turbine structure. We outline an experimental approach to obtain these quantities.

A 1:100 scale model of a Vestas V90 3 MW wind turbine which has a swept area diameter of 90 m and a nacelle height of 105 metres has been developed in BLADE laboratory of the University of Bristol (see Fig. 10 for details). The model wind turbine blades are constructed from a

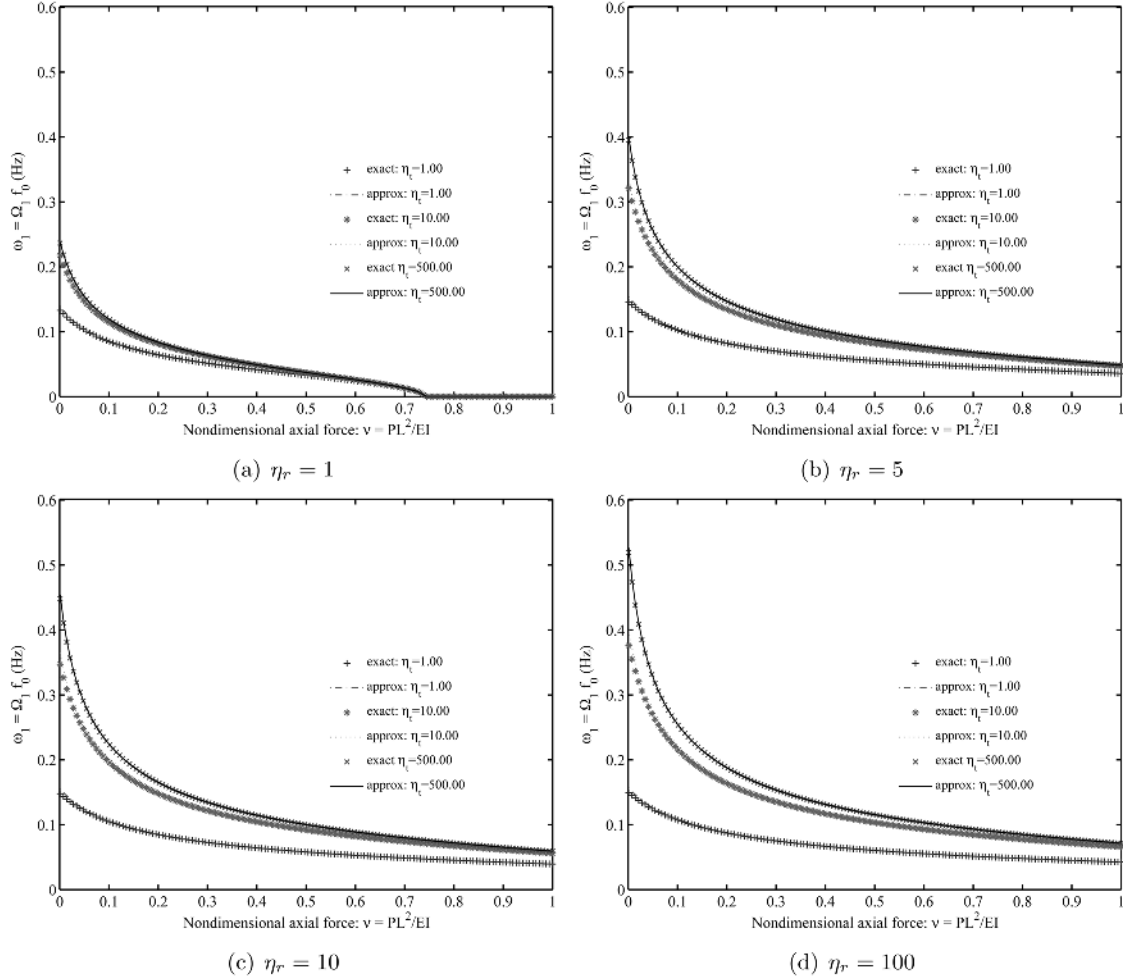


Fig. 8 Approximation of the first natural frequency of the wind turbine with respect to the nondimensional axial load ν for different values of nondimensional translational soil stiffness η_t . Four fixed values of the nondimensional rotational stiffness η_r are considered in the four subplots

lightweight wood and are attached to a 24 v electric motor powered by a DC power supply which is then attached to the tower. The effect of rotor frequency ($1P$) is simulated through the revolutions of the blades powered by the motor. A displacement controlled actuator has been employed which acts at a point in the tower to simulate the wind loading on the structure: mainly the blade passing frequency ($3P$). Monopile type of foundation has been used as shown in Fig. 1. The lateral foundation stiffness (k_t) and the rotational foundation stiffness (k_r) are evaluated by direct measurements as discussed below. The wind turbine was founded on clay. The test procedures adopted to obtain k_r and k_t are as follows:

- *Static moment test to measure k_r* : The rotational stiffness of the foundation (k_r) was measured by applying a moment at the pile head and measuring the slope caused by it.

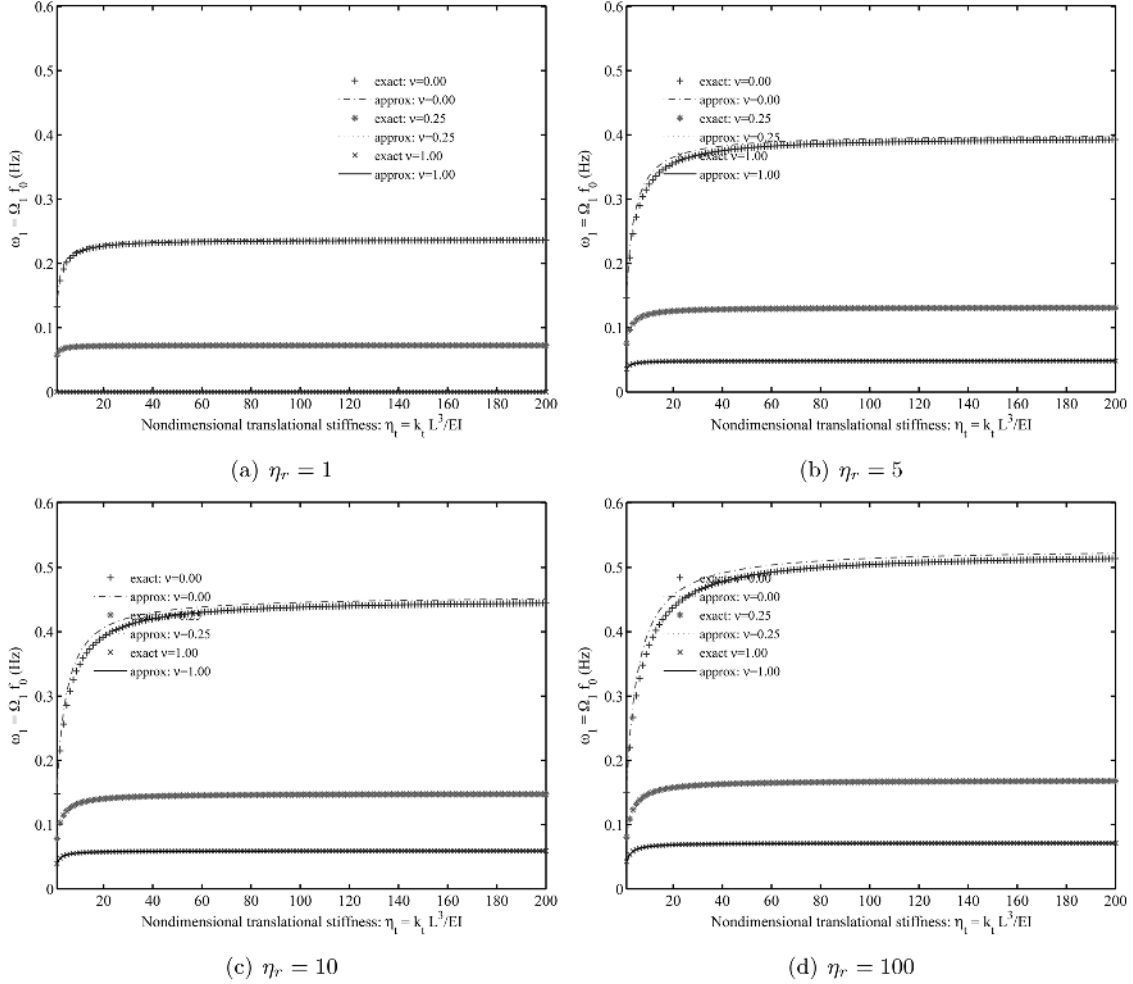


Fig. 9 Approximation of the first natural frequency of the wind turbine with respect to the nondimensional translational stiffness η_t for different values of nondimensional axial load ν . Four fixed values of the nondimensional rotational soil stiffness η_r are considered in the four subplots

The pile was carefully installed in the soil by pushing and was allowed sufficient time to reach steady state. For practical implications see Bhattacharya et al (2009). A known moment was applied at the top of the pile and the rotation of the pile head was obtained by measuring the lateral displacements of two 40 mm spaced dial gauges. Typical results from a test are shown in Fig. 11. The initial tangent is considered as the stiffness as we are interested in small amplitude vibration.

· *Static test to measure k_t* : The horizontal stiffness of the foundation (k_t) was measured by carrying a lateral push over test on the embedded pile in the soil. Lateral load was applied at the top of the pile and the lateral displacements of the pile were measured using a dial gauge. The load displacement curve is plotted and the initial tangent gives the value of k_t . Fig. 12 shows typical test results.

The natural frequency of the wind-turbine system was measured through the free vibration test. This was carried out by applying a small excitation to the system and consequently recording the

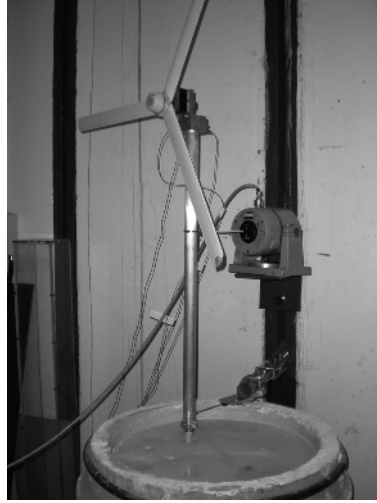


Fig. 10 The model wind turbine embedded in clay. The properties are $-EI$ (Tower): $2.125 \times 10^9 \text{ Nmm}^2$; EI (Pile): $3.18 \times 10^8 \text{ Nmm}^2$; Length of the tower: 1.0 m; Length of the pile (in the clay): 0.5 m

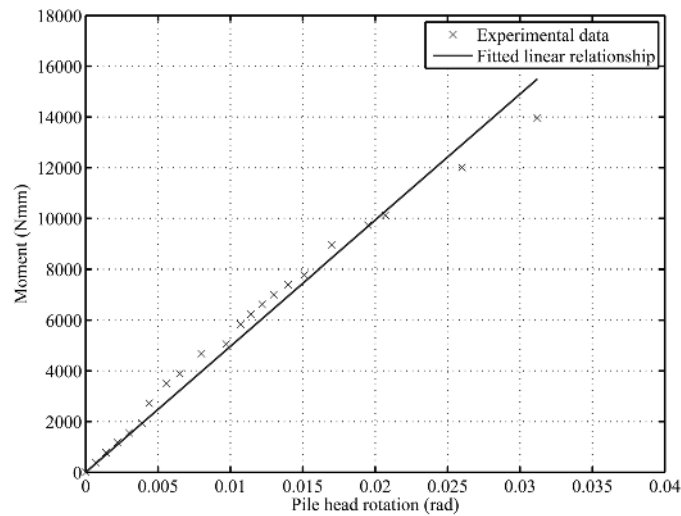


Fig. 11 Experimentally obtained values of k_r for wind turbine founded on clay; linearized value $k_r = 0.428 \text{ MN/mm}$

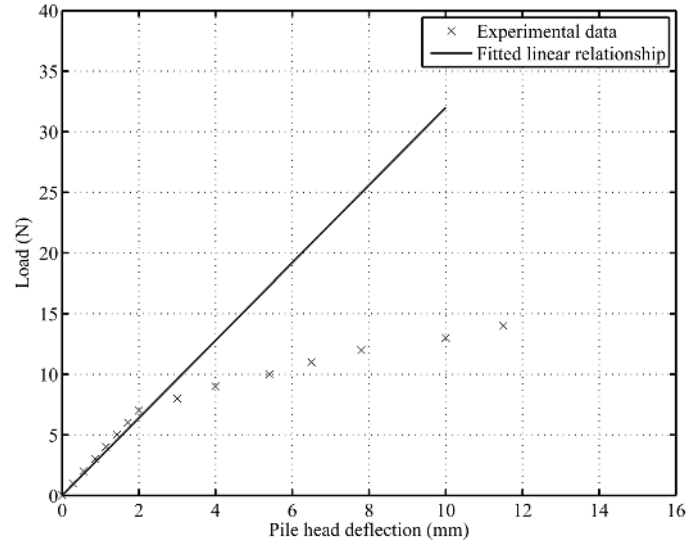
acceleration.

The values of the soil-structure interaction parameters η_r and η_t can be obtained by normalizing k_r and k_t . The nondimensional groups for this experiment are shown in Table 2: Using the nondimensional parameters in Table 2, the correction factors can be determined using Eqs. (70) and (89) as

$$\gamma_k = 0.0547 \quad \text{and} \quad \gamma_m = 0.3637 \quad (97)$$

Table 2 Non-dimensional groups obtained from the experiment

Non-dimensional group	Value	Remarks
$\nu = \frac{PL^2}{EI}$	0.006	Because the value is small, this factor is not very sensitive to the first natural frequency
$\eta_r = \frac{k_r L}{EI}$	0.201	The value of k_r is measured as 0.428MNmm/rad, see Fig. 11.
$\eta_t = \frac{k_t L^3}{EI}$	1.65	The value of k_t is measured as 3.5N/mm, see Fig. 12
$\alpha = \frac{M}{mL}$	2.34	

Fig. 12 Experimentally obtained values of k_t for wind turbine founded on clay; linearized value $k_t = 3.5$ N/mm

Considering the EI of the Tower as 2.125×10^9 Nmm² we have

$$c_0 = \sqrt{\frac{EI}{mL^4}} = \sqrt{\frac{2.125 \times 10^9}{0.5761^4}} = 60.72 \text{ rad/s} \quad (98)$$

Using these, the natural frequency can be obtained from Eq. (47) as

$$f_1 \approx \frac{c_0}{2\pi} \sqrt{\frac{3\gamma_k}{\alpha + \gamma_m}} = 2.3717 \text{ Hz} \quad (99)$$

The measured value of the first natural frequency is 2.35 Hz, which is quite close to the one obtained from the proposed approximate expression.

6.3 Practical application: Lely A2 (500 kW) wind turbine

This has been reported by Zaaier (2006). The wind turbine is NM41 type having 32,000 kg top mass, 41.5 m (L) high and is in with water depth of 4.6 m. The pile is 3.7 m diameter and 20.9 m long with 35 mm wall thickness. The tower is conical having 3.2 m at the base with 1.9 m at the top and is 12 mm thickness. It has been reported that the pile passes through soft layer to stiffer sandy layer.

The tower in the current case is tapered and as the natural frequency formulation is based on uniform tower, an equivalence calculation is necessary to convert the conical tower to a uniform tower. To find out the non-dimensional groups, flexural rigidity (EI) of the tower is necessary for two types of calculations:

1. For the calculation of non-dimensional axial force (ν): This parameter can be replaced by the $\nu =$

$$\frac{PL^2}{EI} = \frac{\pi^2 P}{4 P_{cr}} \text{ where } P_{cr} \text{ is the Euler's elastic critical load. Therefore, this is a buckling type calculation.}$$

A closed form solution can be easily obtained to find the buckling load of a conical cantilever. For the problem in hand, P is 32,000 kg force which is 313.6 MN. The buckling load of this tower (P_{cr}) has been estimated as 17.6 GN.

2. For the calculation of EI for the η_r and η_l , i.e., the foundation parameters, the equivalence is based on stiffness. It can be easily shown that the equivalent second moment of area of a tapering tower (3.2 m base diameter and 1.9 m top diameter and 41.5 m long) of uniform thickness of 12 mm can be replaced by an equivalent 41.5 m long tower of 12 mm thick 2.812 m diameter. The equivalent second I in the calculation is given by

$$I_{eq} = \frac{\pi}{8} \times 2.812^3 \times \frac{12}{1000} = 0.1047 \text{ m}^4 \quad (100)$$

The method to compute the foundation spring constants k_t and k_r can be obtained following Baguelin (1977) and presented by Randolph and Steward (1999). It can be appreciated that the values of k_t and k_r are non-linear and for the natural frequency analysis, only initial values are necessary i.e., the initial slope of the force-pile head displacement graph or the moment-pile head rotation graph. For the current case, as the pile passes through soft layer to stiff layer, a characteristic shear wave velocity of 180 m/s is taken for the soil stiffness calculations. To use the method, it is necessary to find the non-dimensional groups, as evaluated in Table 3. Using the non-dimensional parameters in Table 3, the correction factors can be determined using Eqs. (70) and (89) as

$$\gamma_k = 0.9274 \text{ and } \gamma_m = 0.2417 \quad (101)$$

Considering the EI of the Tower as $2.125 \times 10^9 \text{ Nmm}^2$ we have

$$c_0 = \sqrt{\frac{EI}{mL^4}} = \sqrt{\frac{2.125 \times 10^9}{0.5761^4}} = 3.13 \text{ rad/s} \quad (102)$$

Using these, the natural frequency can be obtained from Eq. (47) as

Table 3 Non-dimensional groups obtained for the Lely A2 wind turbine

Non-dimensional group	Value	Remarks
$nu = \frac{PL^2}{EI} = \frac{\pi^2 P}{4 P_{cr}}$	0.00005	This factor is not very sensitive to the first natural frequency
$\eta_r = \frac{k_r L^3}{EI}$	38.88. The following values has been taken: $k_r = 20.6$ GNm/rad, $L = 41.5$ m, $E = 210$ GPa, $I = 0.1047\text{m}^4$	The value of k_r is taken as 20.6 GNm/rad
$\eta_t = \frac{k_t L^3}{EI}$	2698. The following values has been taken: $k_t = 830$ MN/m, $L = 41.5$ m, $E = 210$ GPa, $I = 0.1047\text{m}^4$	The value of k_t is taken as 830 MN/m
$\alpha = \frac{M}{mL}$	1.0178. $M = 32,000$ kg, $mL = 31346$ kg	

$$f_1 \approx \frac{c_0}{2\pi\sqrt{\alpha + \gamma_m}} \sqrt{\frac{3\gamma_k}{\alpha + \gamma_m}} = 0.7404 \text{ Hz} \quad (103)$$

The measured natural frequency of the system is 0.634 Hz, which quite close to the predicted one.

7. Conclusions

The dynamics of flexible turbine towers considering soil-structure interaction have been investigated. The consideration of elastic end supports, used to take account of the soil-structure interaction, is crucial for offshore wind turbines and have received little attention in literature. A distributed parameter based linear dynamic model using the Euler-Bernoulli beam theory with axial load, elastic support stiffness and top mass with rotary inertia is considered. The non-dimensional parameters necessary to understand the dynamic behavior have been identified. These parameters are nondimensional axial force (ν), nondimensional rotational foundation stiffness, (η_r), nondimensional translational foundation stiffness, (η_t), mass ratio between the rotor-blade assembly and the turbine tower (α), nondimensional radius of gyration of the turbine tower (μ). A new closed-form approximate expression for the fundamental frequency of the system has been derived using the energy principles. This expression is a function of two factors, namely the stiffness correction factor (γ_k) and the mass correction factor (γ_m). These two factors in turn are influenced by the soil-structure interaction parameters η_r and η_t . A detailed study has been conducted on the effect of η_r and η_t on the two correction factors.

All the input parameters necessary to use the proposed expression can be obtained from the geometry and material properties of the wind turbine, foundation and soil. Novel experimental methods have been developed to obtain the soil-structure interaction parameters η_r and η_t . Experimental study on clay foundation show that the linear model assumed for η_r and η_t can be used when the rotation and the deflection of the pile-head is small. The proposed closed-form expression is validated using three independent approaches, namely: (a) comparing with the exact numerical solution of the governing characteristic equation, (b) comparing with laboratory-based experiential results and (c) comparing with the measurements from a real wind turbine. Based on the study reported in the paper, we conclude that the proposed closed-form expression can be used as a first

step to obtain the fundamental frequency of wind turbine towers considering the soil-structure interaction into account.

Acknowledgments

SA gratefully acknowledges the support of The Leverhulme Trust for the award of the Philip Leverhulme Prize.

References

- Abramovich, H. and Hamburger, O. (1991), "Vibration of a cantilever timoshenko beam with a tip mass", *J. Sound Vib.*, **148**(1), 162-170.
- Adhikari, S. (1999a), "Modal analysis of linear asymmetric non-conservative systems", *J. Eng. Mech.- ASCE.*, **125**(12), 1372-1379.
- Adhikari, S. (1999b), "Rates of change of eigenvalues and eigenvectors in damped dynamic systems", *J. AIAA*, **37**(11), 1452-1458.
- Adhikari, S. (2004), "Optimal complex modes and an index of damping non-proportionality", *Mech. Syst. Signal Pr.*, **18**(1), 1-27.
- Adhikari, S. and Bhattacharya, S. (2008), "Dynamic instability of pile-supported structures in liquefiable soils during earthquakes", *Shock Vib.*, **15**(6), 665-685.
- Adhikari, S. and Bhattacharya, S. (2011), "Dynamic analysis of wind turbine towers on flexible foundations", *Shock Vib.*
- Baguélin F., Frank R., S. Y. (1977), "Theoretical study of lateral reaction mechanism of piles", *Géotechnique*, **27**, 405-434.
- Bhattacharya, S., Adhikari, S. and Alexander, N. A. (2009), "A simplified method for unied buckling and dynamic analysis of pile-supported structures in seismically liquefiable soils", *Soil Dyn. Earthq. Eng.*, **29**(8), 1220-1235.
- Bhattacharya, S., Carrington, T. and Aldridge, T. (2009), "Observed increases in offshore pile driving resistance", *Proceedings of the Institution of Civil Engineers-Geotechnical Engineering*, **162**(1), 71-80.
- Bhattacharya, S., Dash, S.R. and Adhikari, S. (2008), "On the mechanics of failure of pile-supported structures in liqueable deposits during earthquakes", *Current Science*, **94**(5), 605-611.
- Blevins, R.D. (1984), *Formulas for Natural Frequency and Mode Shape*, Krieger Publishing Company, Malabar, FL, USA.
- Byrne, B. and Houslyby, G. (2003), "Foundations for offshore wind turbine", *Philos. T. R. Soc. A.*, 361.
- Chen, Y. (1963), "On the vibration of beams or rods carrying a concentrated mass", *J. Appl. Mech -T. ASME.*, **30**, 310-311.
- Dash, S.R., Govindaraju, L. and Bhattacharya, S. (2009), "A case study of damages of the Kandla Port and Customs Office tower supported on a mat-pile foundation in liquefied soils under the 2001 Bhuj earthquake", *Soil Dyn. Earthq. Eng.*, **29**(2), 333-346.
- DnV (2001), *Guidelines for design of wind turbines-DnV/Riso*, Code of practice, DnV, USA.
- Elishakoff, I. and Johnson, V. (2005), "Apparently the first closed-form solution of vibrating inhomogeneous beam with a tip mass", *J. Sound Vib.*, **286**(4-5), 1057-1066.
- Elishakoff, I. and Perez, A. (2005), "Design of a polynomially inhomogeneous bar with a tip mass for specied mode shape and natural frequency", *J. Sound Vib.*, **287**(4-5), 1004-1012.
- GHBLADED (2009), *Wind Turbine Design Software*, Garrad Hassan Limited, Bristol, UK.
- Gurgoze, M. (2005a), "On the eigenfrequencies of a cantilever beam carrying a tip spring-mass system with mass of the helical spring considered", *J. Sound Vib.*, **282**(3-5), 1221-1230.
- Gurgoze, M. (2005b), "On the representation of a cantilevered beam carrying a tip mass by an equivalent

- springmass system”, *J. Sound Vib.*, **282**, 538-542.
- Gurgoze, M. and Erol, H. (2002), “On the frequency response function of a damped cantilever simply supported in-span and carrying a tip mass”, *J. Sound Vib.*, **255**(3), 489-500.
- Hetenyi, M. (1946), “Beams on Elastic Foundation: Theory with Applications in the Fields of Civil and Mechanical Engineering”, University of Michigan Press, Ann Arbor, MI USA.
- Huang, T.C. (1961), “The effect of rotatory inertia and of shear deformation on the frequency and normal mode equations of uniform beams with simple end conditions”, *J. Appl. Mech – T. ASME.*, **28**, 579-584.
- IEA (2005), International Energy Statistics 2005: Key World Energy Statistics, International Energy Agency, Paris, France.
- Kreyszig, E. (2006), *Advanced engineering mathematics*, 9th Edition., John Wiley & Sons, New York.
- Laura, P.A.A. and Gutierrez, R.H. (1986), “Vibrations of an elastically restrained cantilever beam of varying cross-section with tip mass of finite length”, *J. Sound Vib.*, **108**(1), 123-131.
- Oz, H.R. (2003), “Natural frequencies of an immersed beam carrying a tip mass with rotatory inertia”, *J. Sound Vib.*, **266**(5), 1099-1108.
- Randolph, M.F. and Steward, D.P. (1999), *Manual for the program PYGM*, University of Western Australia, Australia.
- SAMTECH (2009), SAMCEF for Wind Turbine (S4WT), SAMTECT s.a., Liege, Belgium.
- Sheu, G. and Yang, S. (2005), “Dynamic analysis of a spinning rayleigh beam”, *Int. J. Mech. Sci.*, **47**(2), 157-169.
- Tempel, D.P. and Molenaar, D.P. (2002), “Wind turbine structural dynamics -a review of the principles for modern power generation, onshore and offshore”, *Wind Eng.*, **26**(4), 211-220.
- Wu, J.S. and Chou, H.M. (1998), “Free vibration analysis of a cantilever beam carrying any number of elastically mounted point masses with the analytical-and-numerical-combined method”, *J. Sound Vib.*, **213**(2), 317-332.
- Wu, J.S. and Chou, H.M. (1999), “A new approach for determining the natural frequencies and mode shapes of a uniform beam carrying any number of sprung masses”, *J. Sound Vib.*, **220**(3), 451- 468.
- Wu, J.S. and Hsu, S.H. (2006), “A unified approach for the free vibration analysis of an elastically supported immersed uniform beam carrying an eccentric tip mass with rotary inertia”, *J. Sound Vib.*, **291**(3-5), 1122-1147.
- Zaaijer, M. (2006), “Foundation modelling to assess dynamic behaviour of offshore wind turbines”, *Appl. Ocean Res.*, **28**, 45-57.

CC

Nomenclature

α	mass ratio, $\alpha = \frac{M}{mL}$
β	nondimensional rotary inertia, $\beta = \frac{J}{mL^3}$
η_r	nondimensional rotational end stiffness, $\eta_r = \frac{k_r L}{EI}$
η_t	nondimensional translational end stiffness, $\eta_t = \frac{k_t L^3}{EI}$
γ_k	stiffness correction factor, $\gamma_k = \frac{k_e}{k_{CL}}$
γ_m	mass correction factor
μ	nondimensional radius of gyration, $\mu = \frac{r}{L}$

ν	nondimensional axial force, $\nu = \frac{PL^2}{EI}$
Ω	nondimensional frequency parameter, $\Omega^2 = \omega^2 \frac{mL^4}{EI}$
ω	angular frequency (rad/s)
ξ	non-dimensional length parameter, $\xi = x/L$
c_0	natural frequency scaling parameter (s^{-1}), $c_0 = \sqrt{\frac{EI}{mL^4}}$
EI	bending stiffness of the beam
$F(\xi)$	transverse force on the beam
$f(x, t)$	applied time dependent distributed load on the beam
f_i	natural frequency (Hz)
J	rotary inertia of the rotor system
k_e	equivalent end stiffness of the beam
k_r	rotational end stiffness of the elastic support
k_t	translational (linear) end stiffness of the elastic support
k_{CL}	equivalent end stiffness of a cantilever beam, $k_{CL} = \frac{3EI}{L^3}$
L	length of the beam
M	mass of the rotor system
m	mass per unit length of the beam, $m = \rho A$
M_b	mass of the beam, $M_b = mL$
M_e	equivalent mass of the SDOF system
P	constant axial force in the beam
r	radius of gyration of the beam
t	time
$W(\xi)$	transverse deflection of the beam
$w(x, t)$	time depended transverse deflection of the beam
x	spatial coordinate along the length of the beam
(\bullet)	derivative with respect to the spatial coordinate
$(\bullet)^T$	matrix transposition
$(\dot{\bullet})$	derivative with respect to time
(\bullet)	determinant of a matrix